ELSEVIER

Physica C 340 (2000) 101–111

PHYSICA C

www.elsevier.nl/locate/physc

Sinter-forging conditions, texture and transport properties of Bi-2212 superconductors

R. Caillard [a,*], V. Garnier [b], G. Desgardin [b]

[a] *Laboratoire LERMAT, ISMRa, 6 Bd. du Marechal Juin, 14050 Caen Cedex, France*
[b] *Laboratoire CRISMAT, 6 Bd. Marechal Juin, 14050 Caen Cedex, France*

Received 8 March 2000; received in revised form 22 May 2000; accepted 5 June 2000

Abstract

The optimization of the sinter-forging process of the Bi–Sr–Ca–Cu–O (2212) superconducting ceramic, synthesized by a polymer matrix method has been done. The precursor powder was pressed under uniaxial stresses ranging between 15.9 and 46.8 MPa, and heated between 830°C and 845°C. Rather well textured samples showing less than 5.6 disorientation degrees for 50% of the grain respect to the *ab* plane have been obtained. The relationships between the stress value as well as the sinter-forging temperature and the samples texture have been correlated with the critical current densities, J_c, at 77 K. Maximum J_c close to 700 A cm^{-2} have been achieved with a pressure of 31.4 MPa and a temperature of 840°C showing that annealing under O_2/N_2 has also to be optimized to obtain in such sinter-forged bulk materials higher J_c values.

Keywords: $Bi_2Sr_2CaCu_2O_8$; Sinter-forging; Texture; Critical current density

1. Introduction

It is well known that high-temperature superconductors have limited superconducting properties because of their intergranular junctions inducing weak links and have to be textured in order to exhibit high critical current densities. The texturing process induces grains alignment according to the *ab* plane and improves intergranular junctions, which is essential to get samples with high critical current densities. The sinter-forging processes used in the literature for Bi-based materials involve large temperature range (from 810°C [18] to 870°C [19]), large applied pressure range (from 3 MPa [20] to 10 MPa [21]) and could present two different consecutive sinter-forging step conditions [22,23]. Using this technique, the 2223 phase has much more been studied up to now than the 2212 one, because of its better electrical properties. Nevertheless, the 2223 phase formation kinetics is sluggish when compared to the 2212 one. Few sinter-forging articles using the 2212 phase have been written and from our knowledge, no sinter-forging condition optimization has been performed for the 2212 phase. However, some authors [1,24] use an applied pressure of 6 MPa and a sinter-forging temperature of 845°C and 850°C.

* Corresponding author. Tel.: +33-2-3145-2672; fax: +33-2-3145-2660.
E-mail address: caillard@labolermat.ismra.fr (R. Caillard).

0921-4534/00/$ - see front matter
PII: S0921-4534(00)01320-4

In this work, both pressure and temperature parameters applied in a sinter-forging process have been optimized. The effects of the sinter-forging conditions on intrinsic properties (e.g. grain orientation) and on extrinsic properties (transport critical current density) have been discussed.

2. Experimental procedure

Powders with the nominal composition $Bi_2Sr_2CaCu_2O_{8+\delta}$ have been prepared using a polymer matrix method [25]. The precursors, $Bi(CH_3COO)_3$ (Aldrich, <99.99%), $Sr(CH_3COO)_2 \cdot (1/2)H_2O$ (Aldrich, <99.9%), $Ca(CH_3COO)_2 \cdot H_2O$ (Aldrich, 99%) and $Cu(CH_3COO)_2 \cdot H_2O$ (Aldrich, <98%) were dissolved in a mixture of acetic acid (SDS, 99%) and distilled water to obtain a pale blue solution. To this solution, another solution ofpolyethyleneimine (PEI Aldrich, 50 wt.% H_2O) in distilled water was added and the resulting solution turned royal blue immediately. This dark blue solution was then introduced into a rotary evaporator to reduce the volume to approximately 10% of the initial volume. As described in our previous work [25], the concentrated solution is fired in a hot plate at 400°C and milled. The resulting powder is calcined in two steps, first at 750°C for 6 h and secondly at 800°C for 6 h with an intermediate milling. After cooling, the remaining powder is ground to obtain an average powder grain size close to 2.5 μm and pelletized under uniaxial pressure (200 MPa, 16 mm diameter, ~3 g, 5 mm thickness). The green density obtained is more than 60% of the theoretical one. After sintering at 845°C for 12 h, the X-ray pattern (Fig. 1) shows principally the 2212 phase, with the presence of secondary phases ((Sr, Ca)CuO and CuO) in small amount (low-intensity peaks). The pellets were then set in a shell furnace (Fig. 2) between two 0.1 mm thick silver foil to prevent any reaction with the alumina rods during sinter forging. The sinter-forging conditions, controlled by temperature, stress and time were chosen to allow an easy separation of the final disc from the silver foil. The sinter-forging temperature was measured with a Pt–PtRh thermocouple placed close to the sample and adjusted before each sinter-

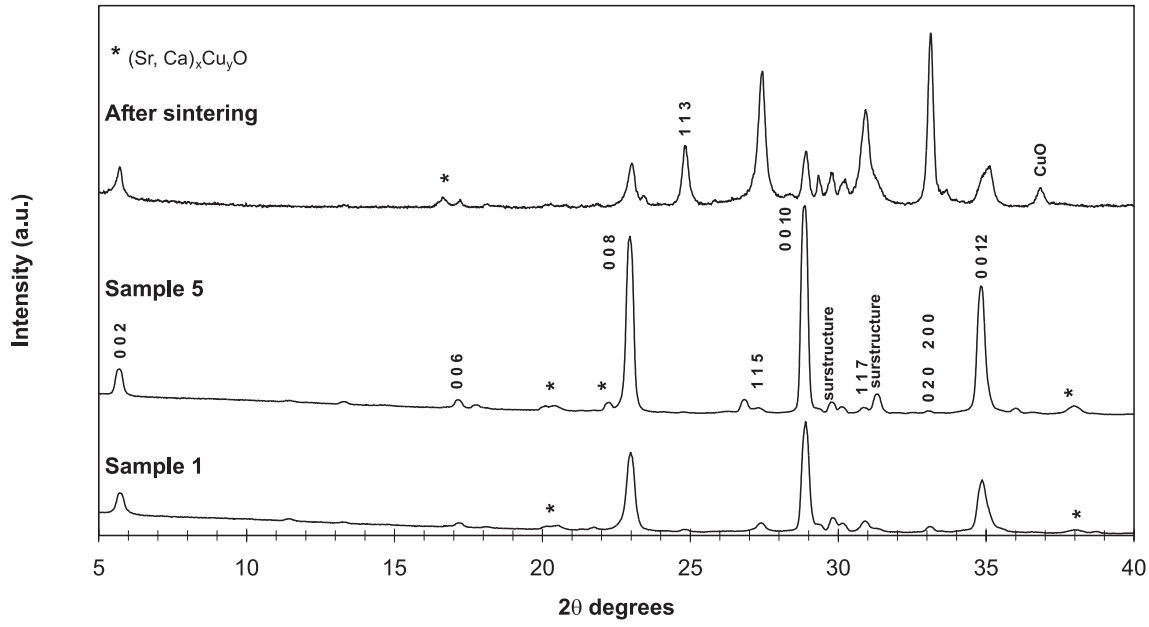

Fig. 1. X-ray diffraction of sinter-forged samples for the worst, sample 1 (835°C/15.9 MPa), and the best, sample 5 (835°C/31.4 MPa), and after sintering 845°C/12 h.

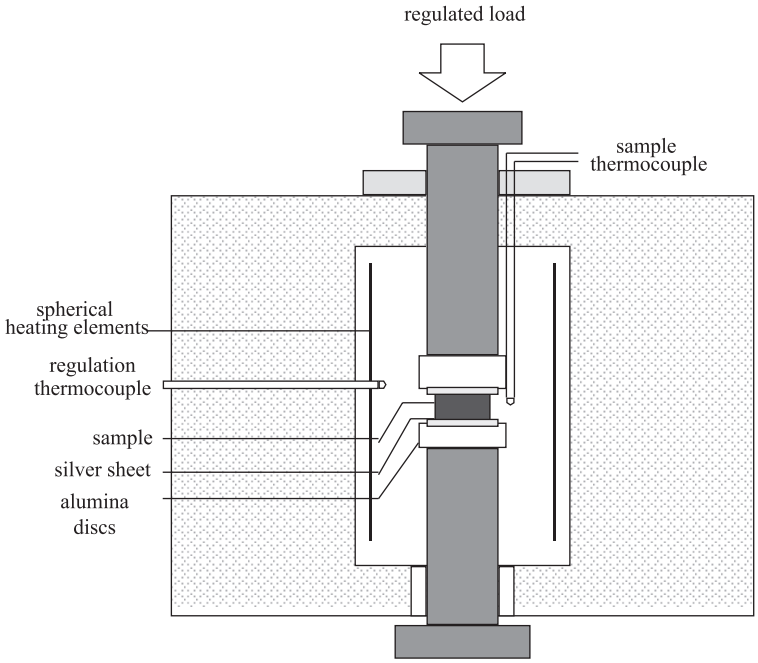

Fig. 2. Schematic view of the hot-forging apparatus.

forging experiment. The pressure has been controlled by a force sensor FGP instrumentation.

The sinter-forging process is controlled through stress ramp and dwell as schematically described in Fig. 3. The stress range is between 15.1 and 46.8MPa. The temperature used for the whole study is constant when pressing, and ranges between 830°C and 845°C. This range of temperature allows a priori the pellets to be easily removed from the silver sheets. Above 845°C, the sample decomposition leads to a too important liquid phase formation and gives large inhomogeneity, not allowing the sample separation from the silver foil without breaking it. Pressure is released before decreasing the temperature to avoid cracks in the Bi-2212 discs which could be caused by the linear expansion coefficient difference between the sample and the Ag sheets.

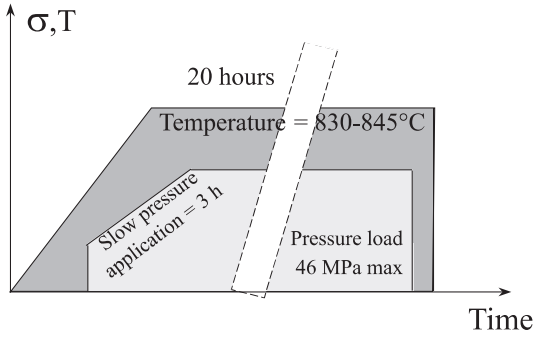

Fig. 3. Schema of the sinter-forging cycle pressure versus time performed on sintered 2212 pellets at different temperatures.

The furnace is turned off and the temperature decreases at 10°C per minute to set the disc state and to avoid any 2212 decomposition into 2201 which can occur with a slow cooling [19–26]. Pole figures measurements were performed on the (0 0 12) reflection using an X-ray diffractometer.

After sinter forging, the pellets were cut into sticks (1.5×15 mm^2) (thickness dimensions are given in Table 1). Thus, bars cut from the discs were silver threaded and welded by a silver past before a post-annealing at 820°C for 50 h in either, 7.5% O_2/balance N_2 followed by a slow cooling rate (2°C per hour) down to 780°C, and before quenching down to room temperature,

Table 1
Summary of the main characteristics of the investigated samples

Sample number	Sinter-forging pressure (MPa)	Sinter-forging temperature (°C)	Texture quality[a] (deg)	Thickness (mm)	T_c (K) after annealing under air	J_c (A cm^{-2}) after annealing under air	T_c (K) after annealing under 7.5% O_2	J_c (A cm^{-2}) after annealing under 7.5% O_2
1	15.9	830	7.6	1.10	85.5	180	86.5	250
2	23.6	830	7.5	1.03	86	350	87	390
3	31.4	830	7.25	0.84	86	430	87	470
4	46.8	830	6.3	0.80	86	390	87	495
5	31.4	835	5.55	0.80	88	440	88.5	540
6	31.4	840	6.5	0.69	88	685	89	710
7	31.4	845	7.15	0.83	88	640	89	695

[a] Misorientation for 50% of the grains.

according to a previous study on textured materials obtained by Park et al. [22], or under air at 820°C for 50 h and then directly quenched down to room temperature.

For resistivity and transport current measurements, a Superconducting Quantum Interference Design (SQUID) magnetometer was used and the transport current density was determined from the DC current–voltage curve using a 1 μV cm^{-1} criterion with a four-probe method.

3. Texture characterization

Pole figure measurements were performed on each sinter-forged sample. All the disorientation

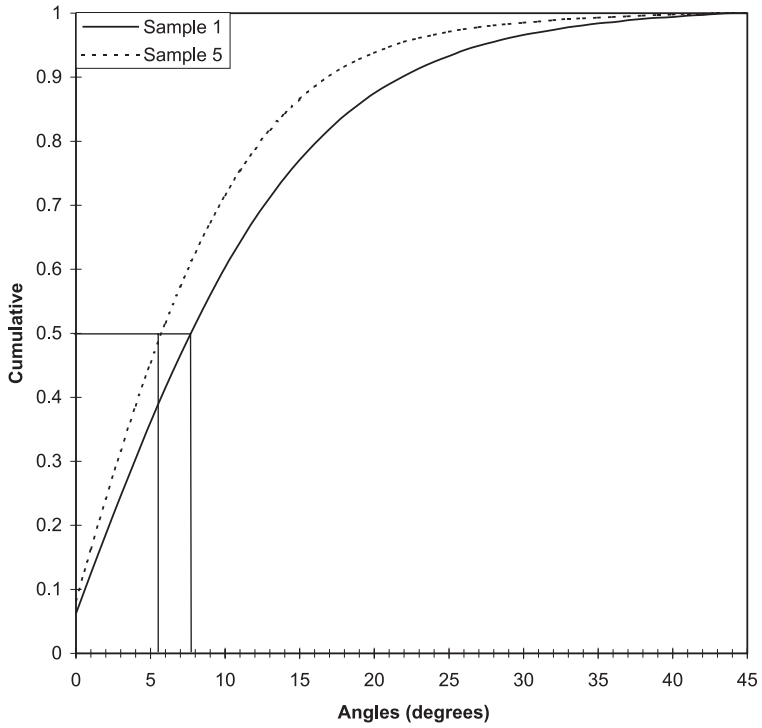

Fig. 4. Cumulative curves showing that 50% of the grains are aligned within 5.55° and 7.6° for samples 5 and 1, respectively.

data are summarized in Table 1. Cumulative curves (Fig. 4) show the best and the worst grain alignment results, corresponding to samples 5 and 1 with less than 5.55 and 7.6 disorientation degrees for 50% of the grains, respectively. XRD patterns obtained using the same measurement conditions are shown in Fig. 1. Both spectra (samples 1 and 5) show that the Bi-2212 phase is still pure excepted additional peaks due to the formation of (Sr, Ca)CuO secondary phases along the sinter-forging process. Spectra for sample 5 exhibit higher (0 0 1) peaks intensities than spectra for sample 1, with narrow full width half maximum of the peaks, showing a better texture and crystallinity for sample 5. In Fig. 5, the SEM micrographs confirm the texture difference between samples 1 and 5. Sample 5 shows that the grains are better oriented and better joined than sample 1. Fig. 6 points out

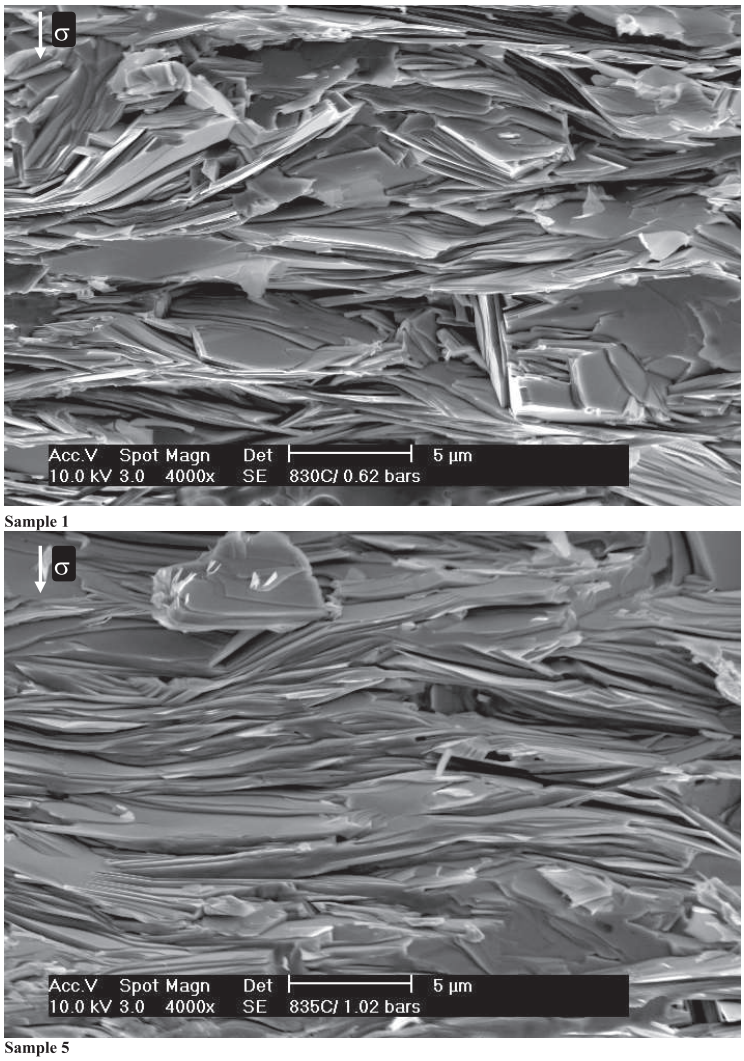

Fig. 5. SEM micrographs of annealed bars after sinter-forging samples at 840°C/31.4 MPa and 835°C/15.9 MPa. The arrow shows the direction of the applied pressure.

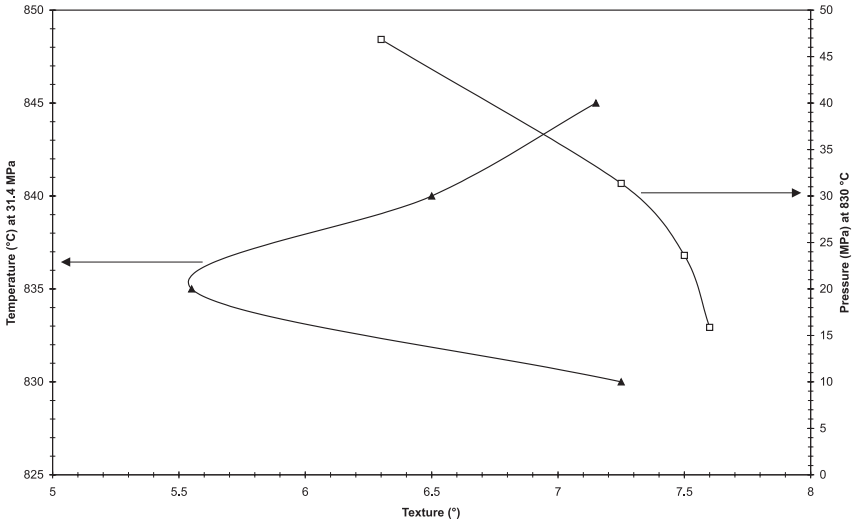

Fig. 6. Texture versus temperature (at 31.4 MPa) and pressure (at 830°C).

the texture evolution with the sinter-forging temperature at 31.4 MPa and with the sinter-forging pressure at 830°C, respectively. In the first case, with a constant pressure of 31.4 MPa, the texture reaches its optimum at 835°C. At 830°C, the texture is only 7.6° because the liquid phase is too viscous and not largely formed to let the grains swiping and orienting on each other. At 835°C, the liquid phase being in larger quantity with a lower viscosity, the grain alignment is favored. If the temperature increases (840°C and 845°C) the liquid phase becomes more and more important and less and less viscous leading to its rapid migration under the pressure toward the sample external part, and so, to a worse texture and inhomogeneity. In the second case, under the same temperature of 830°C, the grain disorientation decreases as the pressure increases. When the pressure is low and increases from 15.9 to 31.4 MPa, the texture is only improved from 7.6° to 7.25° respectively. Also as the pressure reaches 46.8 MPa, the texture is largely improved with less than 6.3° of disorientation for 50% of the grains. However, this high-pressure value does not allow the total recovery of the sample, because it is pasted and has reacted with the Ag sheet. In Table 1 are also reported the samples thickness after sinter-forging (the starting thickness was 5 mm for all the samples, as notified previously). Showing that the lower the thickness is, the better the texture, indicating that more the sample has been flatting and deform, higher the texture is, as expected a priori.

In conclusion, all the samples performed are rather well textured from 7.6° to 5.55°, whatever be the sinter-forging conditions. The best textured sample is obtained at the temperature of 835°C and the pressure of 31.4 MPa (i.e. sample 5), allowing an easy separation of this sample from the Ag sheet. But, even if the sinter-forging parameters are optimized according to the texture viewpoint, the importance of electrical properties could not be occulted. Section 4 is devoted to the superconducting properties of the so-textured samples.

4. Electrical properties

Electrical properties are known to depend on the texture quality [14]: with similar grain boundaries, the best the grain alignment, the higher the J_c is. Therefore, it is important to obtain the best

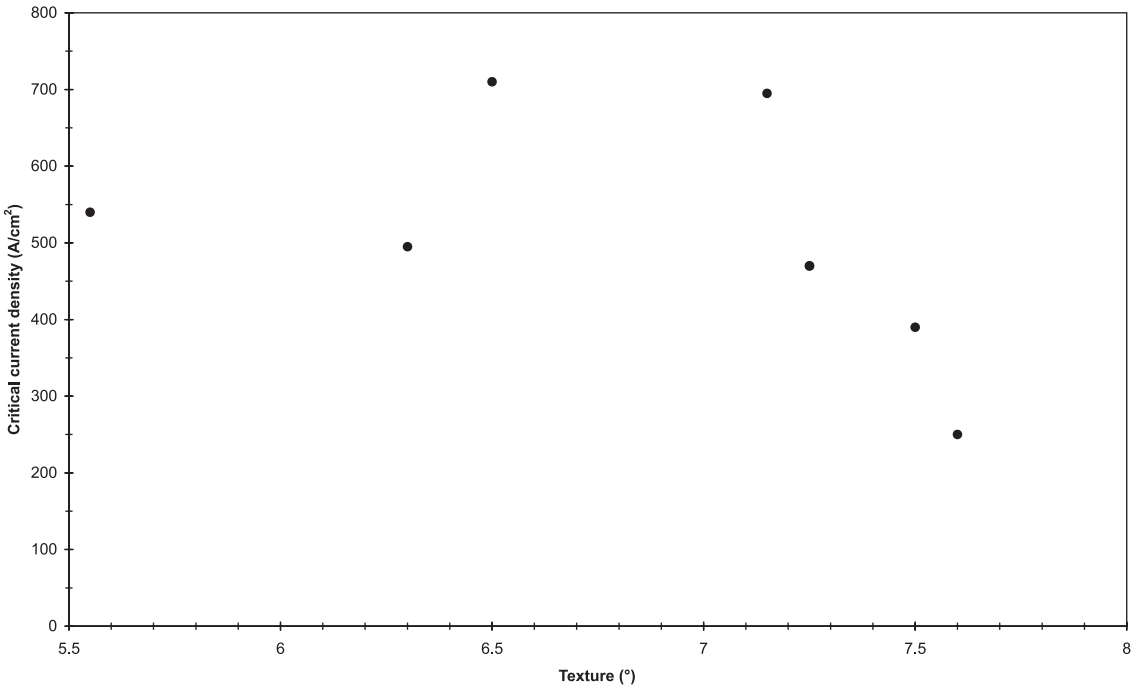

Fig. 7. Critical current density versus texture.

textured samples as possible. Fig. 7 shows samples J_c at 77 K versus their textures. It is important to notice that J_c does not increase monotonously as grains samples disorientation decreases. Also one can observe a random J_c distribution versus grain orientation. This can be explained by the different sinter-forging parameters (pressure and temperature) which lead to different grain boundary characteristics, and then to different J_c values. In any way, our grains samples disorientation is too close from each other (between 5.55° and 7.6°) to conclude a significant dependence of J_c variation with the grain alignment. Fig. 8 points out the J_c dependence with the applied pressure, using the same sinter-forging temperature of 830°C. The J_c rises rapidly until the pressure reaches 31.4 MPa; then, as the pressure increases to 46.8 MPa, the J_c practically does not change from 470 to 495 $A\,cm^{-2}$. The texture improvement, shown in Fig. 6, as the pressure increases, can explain this J_c increase, except for sample 4, sinter forged at 46.8 MPa which is partially pasted with the Ag sheet and does not allow the good exploitation of this highly pressed bulk. Therefore, we choose to fix the pressure at 31.4 MPa for the following experiments, when varying the sinter-forging temperature. Fig. 9 shows the J_c evolution when changing the sinter-forging temperature, but using the same sinter-forging pressure of 31.4 MPa. All the samples were both annealed under air and under 7.5% $O_2 + 92.5\%$ N_2. For all of the annealed samples under 7.5% $O_2 + 92.5\%$ N_2, the J_c are better than those annealed under air (Figs. 8 and 9), about 15% more on average. In the samples annealed under O_2, the J_c is improved from 470 to 710 $A\,cm^{-2}$ as the temperature increases from 830°C to 840°C. At 840°C, the J_c reaches its maximum and then slightly decreases as the temperature rises to 845°C. The texture grade being not related to the J_c level, one can explain this result by an improvement of the grain boundaries when the temperature rises from 830°C to 840°C, leading to a better J_c. On the contrary, the sinter-forging process decreasing the material melting point [19],

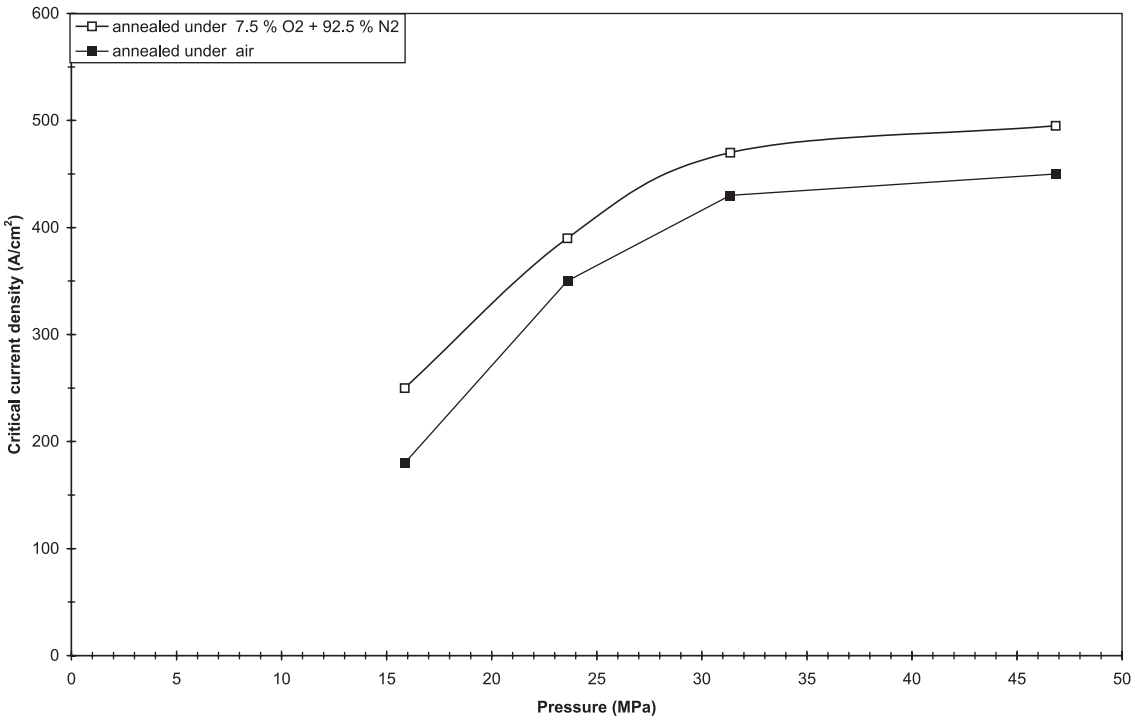

Fig. 8. Critical current density versus pressure at 830°C.

some decomposition occurs at 845°C decreasing the J_c under the influence of high applied pressure: the 2201 phase takes place at the grain boundaries as already shown by Murayama et al. [27] using TEM observations. It has effectively been established that a residual 2201 phase can reduce the critical current by a factor of 2 [28] and degrades the grain connectivity [29]. Fig. 9 shows likewise an improvement of the T_c when the samples are annealed under 7.5% $O_2 + 92.5\%$ N_2. The T_c follows the same kind of variation than the J_c with temperature. The maximum is obtained for 840°C with a T_c of 89 K.

However, a large T_c transition, leading from 70 to 85 K is observed (Fig. 10). This can explain our relatively poor critical current density results since our J_c values have been measured at 77 K, that is to say, in the middle of the T_c transition. This wideness of the transition could be caused by O_2 vacancies, so one can think that J_c could be further improved by a better annealing, and could lead to a 2201 phase content reduction at the grain boundaries.

5. Conclusion

The effects of the sinter-forging parameters (pressure, temperature) on the texture and on the superconducting properties have been studied. Using the same sinter-forging temperature, it has been shown that the texture is improved when the pressure increases. But for high pressure J_c nearly does not increase, and a too high pressure (45 MPa) does not allow a total sample recovery. This implies that, the pressure induces a better grain orientation, but does not improve compulsory the grain boundaries. Using the same pressure of 31.4 MPa, at 845°C, the phase started to decompose, and the J_c goes down. Therefore, the optimal temperature has been found to be 840°C, when using an optimal pressure of 31.4 MPa, leading to

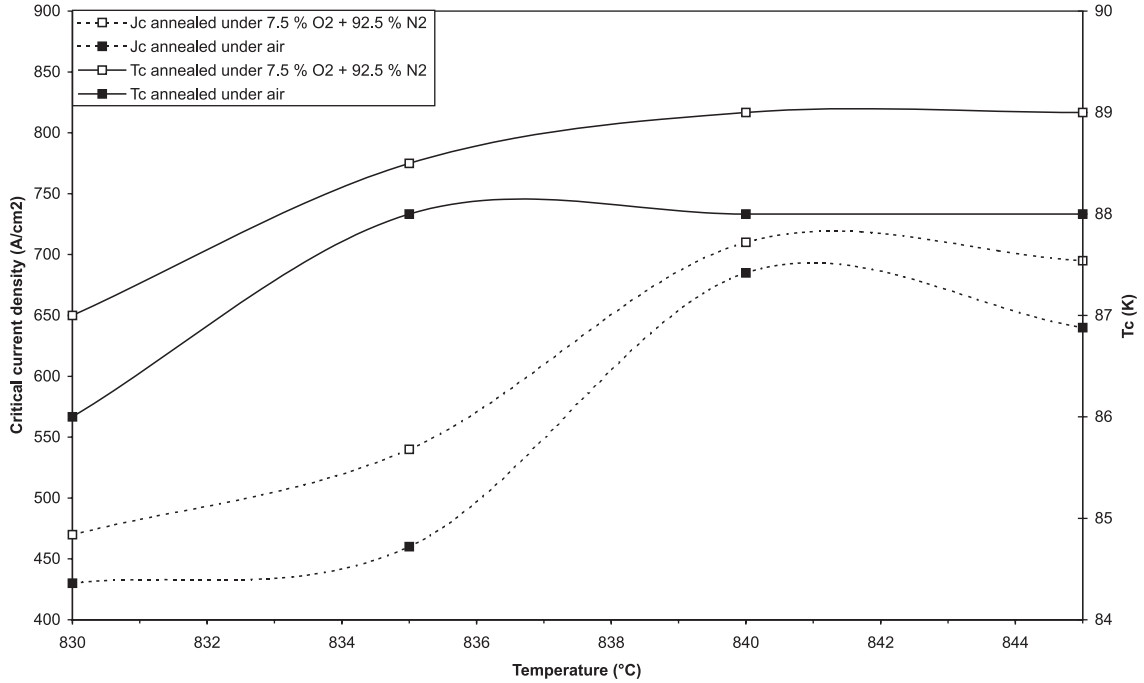

Fig. 9. Critical current transport density, J_c, versus temperature at 31.4 MPa and critical temperature, T_c, versus temperature at 31.4 MPa.

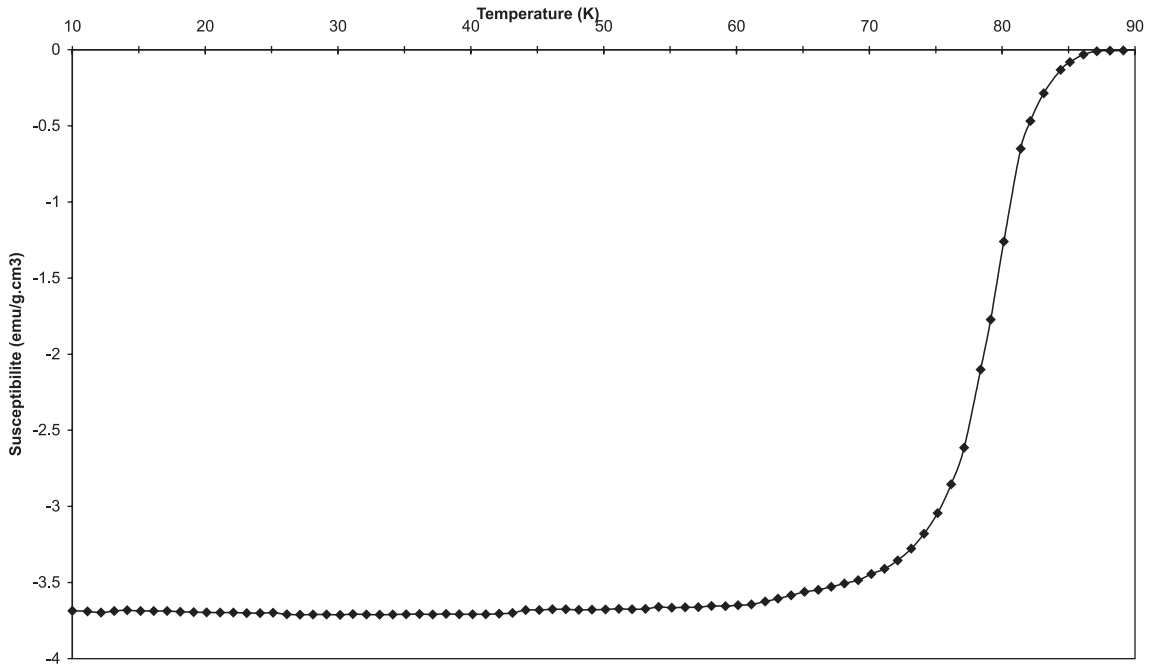

Fig. 10. Susceptibility measurement versus temperature for sample 6 (840°C/31.4 MPa).

a J_c of 710 A cm^{-2}. Annealing under air and under 7.5% O_2 + 92.5% N_2 has been performed, and has shown that the J_c is improved of about 15% and T_c of about 1 K when the samples were annealed under 7.5% O_2 + 92.5% N_2. According to the rather good texture obtained by our sinter-forging method compared to results obtained using lower pressure [2–24] and taking into account the results claimed by different authors for Bi-2212 tapes, we would have expected better transport critical current density, J_c, for this bulk materials. The large superconducting transition observed after annealing for our samples shows that our sinter-forging process, very efficient to texture the material, must be completed by an optimization of the annealing of the ceramics which cannot be traced on the one used for others processes. Optimization of annealing conditions should be done to improve critical current transport density by reducing the 2201 phase amount at the grain boundaries and the T_c transition wideness. In any case, even if our sinter-forged material exhibits relatively low J_c value compared to 2212 Ag-sheated tapes (23 000 A cm^{-2} at 75 K, 0 T [30]), one must consider that the sinter-forging process enable to obtain massive bulk ceramics, different from tapes, which can be useful for current limiters and current lead applications.

Acknowledgements

We thank I. Laffez and S. Marinel for useful discussions and careful reading of the manuscript. We are grateful to G. Poullain for his help in carrying out transport critical current density measurements.

References

[1] H. Seino, K. Ishizaki, M. Takata, Jpn. J. Appl. Phys. 28 (1989) L78.
[2] C.Y. Chu, J.L. Routbort, N. Chen, A.C. Biondo, D.S. Kupperman, K.C. Goretta, Supercond. Sci. Technol. 5 (1992) 306.
[3] D. Berling, J. Beille, B. Loegel, A. Mehdaoui, J.G. Noudem, R. Tournier, Supercond. Sci. Technol. 9 (1996) 205.
[4] J.G. Noudem, J. Beille, E. Beaugnon, D. Bourgault, D. Chateigner, P. Germi, M. Pernet, A. Sulpice, R. Tournier, Supercond. Sci. Technol. 8 (1995) 558.
[5] J.G. Noudem, J. Beille, A. Draperi, A. Sulpice, R. Tournier, Supercond. Sci. Technol. 6 (1993) 795.
[6] A.J. Bourdillon, N.X. Tan, C.L. Ong, J. Mater. Sci. Lett. 15 (1996) 439.
[7] F. Marti, G. Grasso, Y.B. Huang, R. Fluckiger, Supercond. Sci. Technol. 11 (1998) 1251.
[8] Y.T. Zhu, P.S Baldonado, J.F. Binger, T.G. Holesinger, J.O. Willis, D.E. Peterson, Supercond. Sci. Technol. 12 (1999) 640.
[9] W. Pachla, P. Kovac, H. Marciniak, F. Gomory, I. Husek, I. Pochaba, Physica C 248 (1995) 29.
[10] R. Yoshizaki, H. Ikeda, K. Yoshikawa, N. Tomita, Jpn. J. Appl. Phys. 29 (1990) L753.
[11] H. Ikeda, R. Yoshizaki, K. Yoshikawa, N. Tomita, Jpn. J. Appl. Phys. 29 (1990) L430.
[12] N. Murayama, E. Sudo, M. Awano, K. Kani, Y. Torii, Jpn. J. Appl. Phys. 27 (1988) L1856.
[13] M. Kikuchi, T. Atou, H. Hirosaka, K. Fukuoka, Y. Syono, N. Kobayashi, S. Kawamata, K. Okuda, Jpn. J. Appl. Phys. 33 (1994) 6525.
[14] T.V. Mani, A.D. Damodaran, K.G. Warrier, Am. Ceram. Soc. Bullet. 74 (1995) 121.
[15] M. Nevrjva, V. Sima, E. Pollert, J. Cheval, J. Hejtmanek, Preparations and properties of textured BSCCO samples. Chin. J. Phys. 34 (2-II) (1996) Referred version of the contributed paper presented at the Taiwan International Conference on Superconductivity, August 8–11, 1995.
[16] X.K. Fu, V. Rouessac, Y.C. Guo, P.N. Mikheenko, H.K. Liu, S.X. Dou, Physica C 320 (1999) 183.
[17] N. Murayama, J.B. Vander Sande, Physica C 256 (1996) 156.
[18] A. Tampieri, R. Masini, L. Dimeso, S. Guicciardi, M.C. Malpezzi, Jpn. J. Appl. Phys. 32 (1993) 4490.
[19] N. Murayama, W. Shin, Physica C 312 (1999) 255.
[20] N. Chen, A.C. Biondo, S.E. Dorris, K.C. Goretta, M.T. Lanagan, C.A. Youngdahl, R.B. Poeppel, Supercond. Sci. Technol. 6 (1993) 674.
[21] B.L. Fisher, K.C. Goretta, N.C. Harris, U. Balachandran, Critical current densities in Bi-2223 sinter forging. In: Proceeding of the International Cryogenics Materials Conference, July 12–16, 1999.
[22] J.-H Park, K.C. Goretta, N. Murayama, Physica C 312 (1999) 269.
[23] N. Murayama, J.B. Vander Sande, Hot forging with high temperature heat treatment of Bi-Pb-Sr-Ca-Cu-O. In: Proceeding of the Eighth International Symposium on Superconductivity, ISS'95, ISTEC, vol. 2, Advances in Superconductivity VII.

[24] K.C. Goretta, M.E. Loomans, L.J. Martin, J. Joo, R.B. Poeppel, N. Chen, Supercond. Sci. Technol 6 (1993) 282.
[25] V. Garnier, R. Caillard, A. Sotelo, G. Desgardin, Physica C 319 (1999) 197.
[26] H. Liu, L. Liu, Y. Zhang, H. Yu, Z. Jin, J. Mater. Sci 34 (1999) 6099.
[27] N. Murayama, J.B. Vander Sande, Physica C 241 (1995) 235.
[28] Y.C. Guo, J. Horvat, H.K. Liu, S.X. Dou, Physica C 300 (1998) 38.
[29] J. Horvat, Y.C. Guo, B. Zeimetz, H.K. Liu, S.X. Dou, Physica C 300 (1998) 43.
[30] J.O. Willis, R.D. Ray III, T.G. Holesinger, R. Zhou, K.V. Salazou, Bi-2212 and Bi-2223 wire development. In: Proceeding of the 7th US/Japan, Workshop on High temperature Superconductors, Tsukuba, Japan, October 22–24, 1995.